CHAPTER 14

ELASTIC CONSTANTS OF POROUS CERAMICS

Hassel Ledbetter and Ming Lei
Materials Science and Engineering Laboratory, National Institute of Standards and Technology, Boulder, Colorado, USA

S.K. Datta
Department of Mechanical Engineering and CIRES, University of Colorado, Boulder, Colorado, USA

Contents

ABSTRACT

Using theoretical models, we consider the elastic constants of ceramics containing pores. As an example, we consider alumina. However, the approach applies to all ceramics. As a point of departure, we consider spherical pores. For all the usual elastic constants — Young's modulus, shear modulus, bulk modulus, Poisson's ratio — we give relationships for both the forward and inverse cases: predicting the porous ceramic properties and estimating the pore-free ceramic properties. Following a suggestion by Hasselman and Fulrath that sintering or hot pressing can produce cylindrical pores, we derive a relationship for the elastic constants of a distribution of randomly oriented long cylinders ($c/a \to \infty$, the prolate-spheroid limit). This model predicts elastic constants lower than for spherical pores, but well above observation. We obtain agreement with observation by assuming the pores are oblate spheroids. For alumina, the necessary aspect ratio equals one-ninth. Using this oblate-spheroid pore-shape model, we give predictions for all of alumina's elastic constants versus pore volume fraction. Besides pore aspect ratio, the model requires only the pore-free alumina elastic constants. It contains no adjustable parameters.

Handbook of Elastic Properties of Solids, Liquids, and Gases, edited by Levy, Bass, and Stern
Volume III: Elastic Properties of Solids: Biological and Organic Materials, Earth and Marine Sciences

ISBN 0-12-445763-0 / $35.00

14.1. INTRODUCTION

Despite many experimental and theoretical studies, for ceramics there remains a major unsolved problem: how does porosity affect physical properties, especially the elastic constants? When Wachtman [1] reviewed this topic in 1969, he gave 20 references and concluded that nonspherical pores present the principal obstacle to theory.

Since 1969, many more studies have appeared; Phani and Niyogi [2] gave many references. Notable studies include those by Wang [3, 4] and by Sayers and Smiths [5, 6]. Considering uniform-sized spherical particles packed in a cubic array in a porous material, Wang derived a theoretical relationship between porosity and Young's modulus and showed the exact solution graphically. He also proposed an approximate solution that agreed with the exact solution throughout the porosity range 0 to 0.38.

Using a self-consistent theory, Sayers and Smiths [5, 6], calculated the longitudinal-wave velocity for a porous material in the long-wavelength limit. Their calculation applies to the entire range of pore volume fraction, $1 \geq \bar{c} \geq 0$. However, it applies only to spherical pores.

The present study focuses on pore shape. Using methods developed previously and applied to composite materials, we consider the well-understood case of spherical pores. And we consider two further cases. First, an ensemble of randomly oriented rod-shaped (prolate) pores, a geometry suggested by Hasselman and Fulrath [7], but developed incompletely. Second, an ensemble of randomly oriented disc-shaped (oblate) pores. For the present study, we treat a ceramic as a composite containing pores (particles with zero elastic resistance). Related studies were reported by Wu [8], Dean and Lopez [9], Dean [10], Stiffler and Hasselman [11], and Nielsen [12].

14.2. MODELING

We consider pores as "particles" distributed in a homogeneous isotropic matrix. Using a multiple-scattering plane–wave approach, Ledbetter and Datta [13] studied the elastic properties of a composite material containing randomly distributed and randomly oriented ellipsoid-shape particles. They calculated the effective wave speeds of plane waves, both longitudinal and shear, in the long-wavelength limit and gave relationships for the bulk and shear moduli:

$$\frac{B - B_m}{B_p - B_m} = \frac{\dfrac{1}{3}\bar{c} \displaystyle\sum_{i,j=1}^{3} T_{iijj}}{1 - \dfrac{\bar{c}(B_p - B_m)}{3B_m + 4G_m} \displaystyle\sum_{i,j=1}^{3} T_{iijj}} \tag{14.1}$$

$$\frac{G - G_m}{G_p - G_m} = \frac{\dfrac{1}{5}\bar{c}G_m \left(\displaystyle\sum_{i,j=1}^{3} T_{ijij} - \dfrac{1}{3} \sum_{i,j=1}^{3} T_{iijj} \right)}{G_m - \dfrac{2\bar{c}}{75} \dfrac{(G_p - G_m)(3\lambda_m + 8G_m)}{\lambda_m + 2G_m} \left(\displaystyle\sum_{i,j=1}^{3} T_{ijij} - \dfrac{1}{3} \sum_{i,j=1}^{3} T_{iijj} \right)} \tag{14.2}$$

Here, B and $\bar{c}$ denote the bulk modulus and the volume fraction of particles; λ and G denote the Lamé constants. Subscripts m and p denote matrix and particle. Also,

$$T_{ijij} = T_{jiji} = \frac{1}{2(1 + 2US_{ijij})}, \quad \text{for } i, j = 1, 2, 3 \tag{14.3}$$

$$[T_{iijj}] = \begin{bmatrix} 1+US_{1111}+VS_1 & US_{1122}+VS_1 & US_{1133}+VS_1 \\ US_{2211}+VS_2 & 1+US_{2222}+VS_2 & US_{2233}+VS_2 \\ US_{3311}+VS_3 & US_{3322}+VS_3 & 1+US_{3333}+VS_3 \end{bmatrix}^{-1} \tag{14.4}$$

$$U = \frac{G_p}{G_m} - 1 \tag{14.5}$$

$$V = \frac{1}{3}\left(\frac{B_p}{B_m} - \frac{G_p}{G_m}\right) \tag{14.6}$$

$$S_i = \sum_{j=1}^{3} S_{iijj} \tag{14.7}$$

The S_{ijkl} were defined by Eshelby [14] as follows:

$$S_{iiii} = Qa_i^2 I_{a_i a_i} + RI_{a_i} \tag{14.8}$$

$$S_{iijj} = Qa_j^2 I_{a_i a_j} - RI_{a_i} \tag{14.9}$$

$$S_{ijij} = \frac{1}{2}Q(a_i^2 + a_j^2)I_{a_i a_j} + \frac{1}{2}R(I_{a_i} + I_{a_j}) \tag{14.10}$$

where

$$Q = \frac{3}{8\pi(1-\nu)} \text{ and } R = \frac{1-2\nu}{8\pi(1-\nu)} \tag{14.11}$$

and

$$\begin{cases} I_{a_i} = 2\pi abc \int_0^\infty \dfrac{du}{(a_i^2+u)\Delta} \\ I_{a_i a_i} = 2\pi abc \int_0^\infty \dfrac{du}{(a_i^2+u)^2\Delta} \\ I_{a_i a_j} = \dfrac{2}{3}\pi abc \int_0^\infty \dfrac{du}{(a_i^2+u)(a_j^2+u)\Delta} \end{cases} \tag{14.12}$$

with

$$\Delta = \sqrt{(a^2+u)(b^2+u)(c^2+u)} \tag{14.13}$$

Here, ν indicates Poisson's ratio; $a_1 = a$, $a_2 = b$, $a_3 = c$ are ellipsoidal-particle dimensions.

Since for pores the elastic stiffnesses B and G equal zero, in Eqs. 14.1 and 14.2 we put $B_p = G_p = 0$ and obtain

$$B = B_m \left[1 - \frac{\frac{1}{3}\bar{c} \sum_{i,j=1}^{3} T_{iijj}}{1 + \frac{\bar{c}B_m}{3B_m + 4G_m} \sum_{i,j=1}^{3} T_{iijj}} \right] \tag{14.14}$$

$$G = G_m \left[1 - \frac{\frac{1}{5}\bar{c}\left(\sum_{i,j=1}^{3} T_{ijij} - \frac{1}{3}\sum_{i,j=1}^{3} T_{iijj} \right)}{1 + \frac{2\bar{c}}{75}\frac{3\lambda_m + 8G_m}{\lambda_m + 2G_m}\left(\sum_{i,j=1}^{3} T_{ijij} - \frac{1}{3}\sum_{i,j=1}^{3} T_{iijj} \right)} \right] \tag{14.15}$$

Because $U = -1$ and $V = 0$ when $B_p = G_p = 0$,

$$T_{ijij} = T_{jiji} = \frac{1}{2(1+2S_{ijij})} \text{ for } i, j = 1, 2, 3 \tag{14.16}$$

$$[T_{iijj}] = \begin{bmatrix} 1 - S_{1111} & -S_{1122} & -S_{1133} \\ -S_{2211} & 1 - S_{2222} & -S_{2233} \\ -S_{3311} & -S_{3322} & 1 - S_{3333} \end{bmatrix}^{-1} \tag{14.17}$$

14.2.1. Model for Spherical Pores

First, we consider pores as spherical "particles." In this case, $a = b = c$, we obtain

$$\sum_{i,j=1}^{3} T_{iijj} = \frac{9(1 - \nu_m)}{2(1 - 2\nu_m)} \tag{14.18}$$

$$\sum_{i,j=1}^{3} T_{ijij} - \frac{1}{3}\sum_{i,j=1}^{3} T_{iijj} = \frac{75(1 - \nu_m)}{7 - 5\nu_m} \tag{14.19}$$

Substituting Eqs. 14.18 and 14.19 into Eqs. 14.14 and 14.15, and invoking the expressions for elastic constants in terms of bulk and shear moduli, we obtain expressions for the bulk and shear moduli for a material containing spherical pores:

$$B = B_m \frac{4(1 - \bar{c})G_m}{4G_m + 3\bar{c}B_m} \tag{14.20}$$

or

$$B = B_m \left[1 + \frac{A\bar{c}}{1 - (1 + A)\bar{c}}\right] \tag{14.20a}$$

and

$$G = G_m \frac{(1 - \bar{c})(9B_m + 8G_m)}{(9 + 6\bar{c})B_m + (8 + 12\bar{c})G_m} \tag{14.21}$$

or

$$G = G_m \left[1 + \frac{D\bar{c}}{1 - (1 + D)\bar{c}}\right] \tag{14.21a}$$

Here,

$$A = -\frac{3B_m + 4G_m}{4G_m} \tag{14.22}$$

$$D = -\frac{5(3B_m + 4G_m)}{9B_m + 8G_m} \tag{14.23}$$

Equations 14.20 and 14.21 are identical with Hashin's [15] composite-sphere-model equations for the bulk and shear moduli. We invoke the well-known isotropic-material relationships for Young's modulus and Poisson's ratio:

$$E = \frac{9BG}{3B + G} \tag{14.24}$$

and

$$\nu = \frac{1}{2}\frac{3B - 2G}{3B + G} \tag{14.25}$$

For the elastic constants E and ν of a porous material, we obtain

$$E = E_m \frac{4(1 - \bar{c})(3B_m + G_m)(9B_m + 8G_m)}{108B_m^2 + 132B_mG_m + 32G_m^2 + \bar{c}(99B_m^2 + 168B_mG_m)} \tag{14.26}$$

or

$$E = E_m \left[1 + \frac{F\bar{c}}{1 - (1 + F)\bar{c}}\right] \tag{14.26a}$$

and

$$\nu = \nu_m \frac{(3B_m + G_m)\left[36B_m^2 + 8G_mB_m - \frac{64}{3}G_m^2 + \bar{c}\left(6B_m^2 + 32B_mG_m\right)\right]}{(3B_m - 2G_m)\left[36B_m^2 + 44B_mG_m + \frac{32}{3}G_m^2 + \bar{c}\left(33B_m^2 + 56B_mG_m\right)\right]} \tag{14.27}$$

or

$$\nu = \nu_m\left[1 + \frac{H\bar{c}}{1-(1+A)\bar{c}}\right] \tag{14.27a}$$

Here,

$$F = -\frac{207B_m^2 + 300B_mG_m + 32G_m^2}{108B_m^2 + 132B_mG_m + 32G_m^2} \tag{14.28}$$

$$H = -\frac{27B_m(3B_m + 4G_m)(3B_m - 4G_m)}{324B_m^3 + 180B_m^2G_m - 168B_mG_m^2 - 64G_m^3} \tag{14.29}$$

From Eqs. 14.20, 14.21, 14.26, and 14.27, we obtain the inverse relationships:

$$G_m = \frac{-\beta + \sqrt{\beta^2 - 4\alpha\gamma}}{2\alpha} \tag{14.30}$$

$$B_m = \frac{4G_mB}{4(1-\bar{c})G_m - 3\bar{c}B} \tag{14.31}$$

$$E_m = \frac{36G_mB}{4(3B + G_m) - \bar{c}(4G_m + 3B)} \tag{14.32}$$

$$\nu_m = \frac{2(3B - 2G_m) + \bar{c}(4G_m + 3B)}{4(3B + G_m) - \bar{c}(4G_m + 3B)} \tag{14.33}$$

Here,

$$\alpha = \frac{8}{3}(1-\bar{c}) \tag{14.34}$$

$$\beta = (3 - 2\bar{c})B - \left(\frac{8}{3} + 4\bar{c}\right)G \tag{14.35}$$

$$\gamma = -3(1+\bar{c})BG \tag{14.36}$$

We can use Eqs. 14.30–14.33 to estimate the pore-free material properties.

As an example, we choose porous alumina. Table 14.1 shows the physical properties of pore-free alumina obtained from monocrystal elastic constants [16] by a Voigt–Reuss–Hill averaging method. For the Young's modulus of porous alumina, we use the Phani-Niyogi [2] empirical fitting results to Knudsen's [17] measurements. For the Young's modulus, the top curve in Figure 14.1 shows a comparison between measurements and a spherical-pore model. Calculated results for the bulk and shear moduli and Poisson's ratio are shown in the lower parts of Figure 14.1.

14.2.2. Model for Nonspherical Pores

Second, we consider pores as ellipsoidal "particles."

Table 14.1. Properties of nonporous alumina.

ρ (g/cm^3)	E (GPa)	B (GPa)	G (GPa)	λ (GPa)	ν
3.986	402.9	252.1	163.3	143.2	0.2336

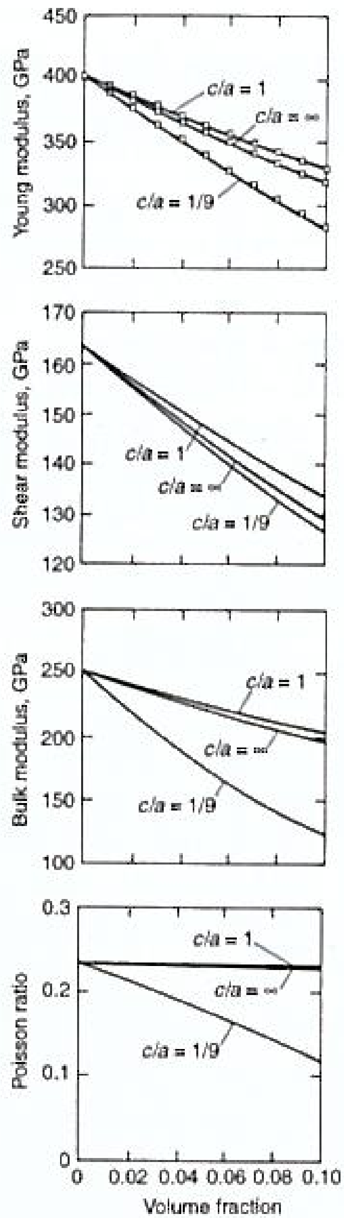

Fig. 14.1. For Young's modulus versus pore volume fraction, this figure compares three sets of modeling results—spheres, prolate-limit cylinders, discs ($c/a = 1/9$)—with observation. Because we fit the disc case to observation, these two curves coincide. Lower curves show bulk modulus, shear modulus, and Poisson's ratio. For Poisson's ratio note coincidence of sphere and prolate-limit cases.

14.2.2.1. Prolate Limit

For a prolate ellipsoid, which approximates a rod, $a = b \ll c$. If we take the limit $c/a \to \infty$, then we get

$$\sum_{i,j=1}^{3} T_{iijj} = \frac{5 - 4\nu_m}{1 - 2\nu_m} \tag{14.37}$$

$$\sum_{i,j=1}^{3} T_{ijij} - \frac{1}{3}\sum_{i,j=1}^{3} T_{iijj} = \frac{8(5 - 3\nu_m)}{3} \tag{14.38}$$

Substituting Eqs. 14.37 and 14.38 into Eqs. 14.14 and 14.15, we obtain expressions for the bulk and shear moduli in the prolate limit:

$$B = B_m \frac{(3B_m + 4G_m)G_m - 4\bar{c}G_m(B_m + G_m)}{(3B_m + 4G_m)G_m + 3\bar{c}B_m(B_m + G_m)} \tag{14.39}$$

or

$$B = B_m \left[1 + \frac{W\bar{c}}{1 - (1 + X)\bar{c}}\right] \tag{14.39a}$$

and

$$G = G_m \frac{75(3B_m + G_m)(3B_m + 4G_m) - 4(21B_m + 16G_m)(9B_m + 8G_m)\bar{c}}{75(3B_m + G_m)(3B_m + 4G_m) + 3B_m(B_m + G_m)\bar{c}} \tag{14.40}$$

or

$$G = G_m \left[1 + \frac{Y\bar{c}}{1 - (1 + Z)\bar{c}}\right] \tag{14.40a}$$

where

$$W = \frac{B_m + G_m}{G_m} \tag{14.41}$$

$$X = -\frac{3B_m^2 + 6B_mG_m + 4G_m^2}{(3B_m + 4G_m)G_m} \tag{14.42}$$

$$Y = -\frac{4(21B_m + 16G_m)}{15(3B_m + G_m)} \tag{14.43}$$

$$Z = -\frac{393B_m^2 + 839B_mG_m + 356G_m^2}{15(3B_m + G_m)(3B_m + 4G_m)} \tag{14.44}$$

Similarly, we can obtain relationships for the Young's modulus and Poisson's ratio by using Eqs. 14.24 and 14.25. For the four principal elastic constants, Figure 14.1 shows the prolate-limit results. Also, in Figure 14.2, we show results calculated for various prolate-spheroid aspect ratios.

14.2.2.2. Oblate Case

Because the prolate-limit-pore-shape approach gives results only slightly below the spherical-pore-shape model and well above observation, we consider oblate-ellipsoid-shape pores ($a = b > c$). The oblate limit ($c/a = 0$) is singular, and we plan to discuss

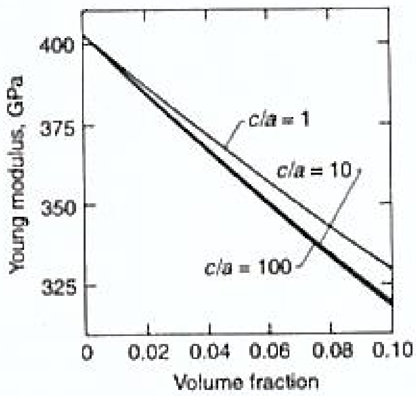

Fig. 14.2. For Young's modulus, effect of aspect ratio of cylindrical (prolate-spheroid) pores. Practically, $c/a \rightarrow \infty$ coincides with $c/a = 100$.

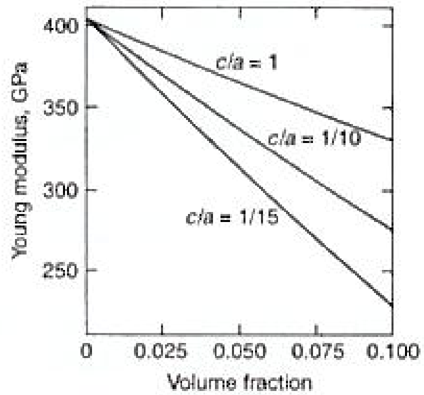

Fig. 14.3. For Young's modulus, effect of aspect ratio of disc-shaped (oblate-spheroid) pores.

elsewhere some analytical expressions for the elastic constants. Here, we give numerical results. Figure 14.3 shows the effect of changing aspect ratio from unity (sphere: $c/a = 1$) toward the oblate limit.

14.3. DISCUSSION

In considering the elastic properties of a porous composite, we take a different approach than that used recently [2–4]. We ignore empirical parameters, particle shape, and particle packing. Instead, we focus on pore geometry. Figure 14.1 shows that the elastic properties depend strongly on the pore shape. And Figures 14.2 and 14.3 show that oblate pores, more than prolate pores, reduce elastic stiffness, depending on pore aspect ratio. Also, for alumina, we see that both spherical and prolate-limit pores fail to agree with observation.

To obtain the best model fit to the observed Young's modulus, we used oblate pores with an aspect ratio of one-ninth. With an aspect ratio less than one-third, oblate pores predict lower bulk and shear moduli and Poisson's ratio than spherical and prolate-limit pores. To check model predictions, for elastic constants other than the Young's modulus, we need measurements of the corresponding properties, measurements generally unavailable.

The theoretical approach described here applies to any material containing voids, not only to porous ceramics. We can also use the model inversely to study pore geometry. Thus, the model provides a possibly valuable nondestructive-evaluation tool. Because the present model fails to allow for pore-pore overlap and because it breaks down for nonspherical particles at high volume concentration [18], we can apply the model only to lower volume fractions. We believe the model can be extended to higher volume fractions. The model ignores the occurrence of, and effect of, microcracks [19].

14.4. CONCLUSIONS

From this study on porous ceramics we reach the following five principal conclusions:

(a) From measurements of the elastic constants of a material containing spherical pores, we can estimate the pore-free material properties by using Eqs. 14.30–14.33.

(b) Physical properties of a porous material depend strongly on the pore shape. Discs produce larger effects than rods.

(c) A model calculation shows that randomly oriented cylinder-shaped pores (even in the prolate limit) predict a too-high elastic stiffness, only slightly lower than for spherical pores.

(d) Theoretical calculations suggest that porous alumina contains oblate-ellipsoid-shaped pores, instead of cylindrical pores suggested by other studies.

(e) Further experimental studies should include elastic constants other than the Young's modulus: for example, Poisson's ratio and bulk modulus. These other elastic constants would provide invaluable checks of predictions made in the present study.

ACKNOWLEDGMENTS

Dr. E. R. Fuller (NIST, Gaithersburg) provided much useful information, reference material, and encouragement.

References

1. Wachtman J.B. pp. 139–168 in *Mechanical and Thermal Properties of Ceramics*, Edited by J.B. Wachtman, Nat. Bur. Stand. (U.S.) Spec. Publ. No. 303, May 1969.
2. Phani, K.K., and Niyogi, S.K. (1987). "Young's modulus of porous brittle solids," *J. Mater. Sci.* **22**: 257–263.
3. Wang, J.C. (1984). "Young's modulus of porous materials, Part I," *J. Mater. Sci.* **19**: 801–808.
4. Wang, J.C. (1984). "Young's modulus of porous materials, Part II," *J. Mater. Sci.* **19**: 809–814.
5. Sayers, C.M. (1981). "Ultrasonic velocity dispersion in porous materials," *J. Phys. D: Appl. Phys.* **14**: 413–420.
6. Sayers, C.M., and Smith, R.L. (1982). "The propagation of ultrasound in porous media," *Ultrasonics* **20**: 201–205.
7. Hasselman, D.P.H., and Fulrath, R.M. (1965). "Effect of cylindrical porosity on Young's modulus of polycrystalline brittle materials," *J. Am. Ceram. Soc.* **48**: 545.
8. Wu, T.T. (1966). "The effect of inclusion shape on the elastic moduli of a two-phase material," *Int. J. Solid Struct.* **2**: 1–8.
9. Dean, E.A., and Lopez, J.A. (1983). "Empirical dependence of elastic moduli on porosity for ceramic materials," *J. Am. Ceram. Soc.* **66**: 366–370.
10. Dean, E.A. (1983). "Elastic moduli of porous sintered materials as modeled by a variable-aspect-ratio self-consistent oblate-spheroidal-inclusion theory," *J. Am. Ceram. Soc.* **66**: 847–854.
11. Stiffler, R.C., and Hasselman, D.P.H. (1983). "Shear moduli of composites with elliptical inclusions," *J. Am. Ceram. Soc.* **66**: C52–C53.
12. Nielsen, L.F. (1984). "Elasticity and damping of porous materials and impregnated materials," *J. Am. Ceram. Soc.* **67**: 93–98.
13. Ledbetter, H.M., and Datta, S.K. (1986). "Effective wave speeds in an SiC-particle-reinforced al composite," *J. Acoust. Soc. Am.* **79**: 239–248.
14. Eshelby, J.D. (1957). "The determination of the elastic field of an ellipsoidal inclusion, and related problems," *Proc. Roy. Soc. Lond.* **A241**: 376–396.
15. Hashin, Z. (1962). "Elastic moduli of heterogeneous materials," *J. Appl. Mech.* **29**: 143–150.
16. W.E. Tefft, (1966). "Elastic constants of synthetic single crystal corundum," *J. Res. Nat. Bur. Stand.* **70A**: 277–280.
17. Knudsen, F.P. (1962). "Effect of porosity on Young's modulus of alumina," *J. Am. Ceram. Soc.* **45**: 94–95.
18. Ledbetter, H.M., Datta, S.K., and Kriz, R.D. (1984). "Elastic constants of an anisotropic, nonhomogeneous particle-reinforced composite," *Acta Metall.* **32**: 2225–2231.
19. Budiansky, B., and O'Connell, R.J. (1976). "Elastic moduli of a cracked solid," *Int. J. Solids Struct.* **12**: 81–97.